X-ray absorption study of Ti-activated sodium aluminum hydride

J. Graetz,[a] J. J. Reilly, and J. Johnson
Department of Energy Sciences and Technology, Brookhaven National Laboratory, Upton, New York 11973

A. Yu. Ignatov and T. A. Tyson
Department of Physics, New Jersey Institute of Technology, Newark, New Jersey 07102

(Received 8 April 2004; accepted 20 May 2004)

Ti *K*-edge x-ray absorption near-edge spectroscopy was used to explore the Ti valence and coordination in Ti-activated sodium alanate. An empirical relationship was established between the Ti valence and the Ti *K*-edge onset based on a set of standards. This relationship was used to estimate oxidation states of the titanium catalyst in 2 and 4 mol % Ti-doped $NaAlH_4$. The results demonstrate that the formal titanium valence is zero in doped sodium alanate and nearly invariant during hydrogen cycling. A qualitative comparison of the edge fine structure suggests that the Ti is present on the surface in the form of amorphous $TiAl_3$. © *2004 American Institute of Physics*. [DOI: 10.1063/1.1773614]

There is currently considerable interest in the development of metal hydrides capable of reversible hydrogen storage at low and medium temperatures. A recent investigation of Ti-doped $NaAlH_4$ by Bogdanovic and Schwickardi has demonstrated reversible cycling in the complex metal hydrides under moderate conditions.[1] Since this discovery there has been considerable work on improving the catalytic effects and understanding the role of the catalyst in the sodium alanates. However, the mechanism by which the $NaAlH_4$ system is activated in the presence of a small amount of Ti is still not well understood. In part, this is because the location and valence of the activating species are unknown.

In sodium aluminum hydride, the hydrogen absorption/desorption occurs through the following two-step decomposition–recombination reaction:

$$NaAlH_4 \leftrightarrow \tfrac{1}{3}Na_3AlH_6 + \tfrac{2}{3}Al + H_2 \leftrightarrow NaH + Al + \tfrac{3}{2}H_2, \quad (1)$$

giving a combined theoretical hydrogen storage capacity of 5.6 wt %. There are a number of possible mechanisms by which a metal dopant might enhance the dehydriding kinetics of Eq. (1).[2] The simplest possibility is that the Ti acts as a classic catalyst and assists the conversion of atomic hydrogen into molecular hydrogen at the surface. This situation is unlikely due to the strong thermodynamic driving force on the Ti to form a hydride in the presence of the desorbed hydrogen.

Another proposed mechanism for the activation of $NaAlH_4$ involves substitution of the dopant in the lattice. A recent x-ray diffraction study of Ti and Zr-doped $NaAlH_4$ has demonstrated lattice distortions associated with doping the hydride.[3] Based on these distortions, Sun *et al.* have suggested that the Ti is substituted for the Na cation[3,4] and is present as Ti^{4+} at doping levels $\leqslant$2 mol %. The enhanced kinetics are attributed to vacancy formation and the lattice distortion associated with the bulk lattice substitution.

A final possibility is that the hydrogen diffuses to the surface in an Al–H complex where it is dissociated by the catalyzing agent and releases H_2. This process leads to significant coalescence of Al on the particle surface in the dehydrided state. Energy dispersive spectroscopy of Ti-doped $NaAlH_4$ has revealed Al segregation towards regions of higher Ti concentration on the particle surface upon the initial dehydrogenation.[5] The presence of zero-valent Ti is also supported by H_2 evolution during the doping process.[1,6] Other investigations of Ti-activated sodium alanate have demonstrated the formation of a $TiAl_3$ phaseupon ball milling a 3:1 mixture of $NaAlH_4$ and $TiCl_3$.[7] However, it has been shown that only *2* mol % of the metal is required to activate $NaAlH_4$.[4,8,9] Therefore, studies of excessively doped $NaAlH_4$ yield properties of the excess metal and not the activating species.

This letter presents x-ray absorption spectroscopy measurements of the Ti *K* edge from the 2 and 4 mol % Ti-doped $NaAlH_4$. The Ti valence was determined using the x-ray absorption near-edge structure.

Ti-doped $NaAlH_4$ was prepared by mechanically milling 95% pure $NaAlH_4$ (Alfa) with $TiCl_3$ (Aldrich 99%) in a Fritsch Pulverisette 6 planetary mill. The powders (~1.2 g) were milled in a 250 ml tungsten carbide bowl using seven 15 mm diam WC balls (~26 g each). Mechanical attrition was performed in an inert Ar atmosphere for 1.5 h. Samples containing 2 and 4 mol % $TiCl_3$ were prepared for this study. The Ti-doped materials were cycled through the two-step reaction of Eq. (1) four times in a calibrated fixed volume to ensure a homogeneous Ti distribution. $TiH_{1.1}$ was prepared by dehydriding TiH_2 (Alfa 99%) at 700 °C into a calibrated fixed volume. $TiAl_3$, $Ti_{0.08}Al_{0.92}$, and $Ti_{0.02}Al_{0.98}$ were prepared by arc melting the components in a He atmosphere. The FeTi and $TiAl_3$ were crushed into a powder, while the more ductile alloys of $Ti_{0.08}Al_{0.92}$ and $Ti_{0.02}Al_{0.98}$ were pressed into thin pellets (123 MPa). Other Ti-containing materials included powders of TiO (Alfa 99.5%), Ti_2O_3 (Aldrich 99.9%), TiO_2 containing a mixture of anatase and rutile phases (Johnson Matthey 99.995%), FeTi (Canon-Muskegon 99%), $TiCl_3$ (Aldrich 99.999%), and TiH_2 (Alfa 99%), and Ti metal foil (Materials Research Corp. 99.97%). All powders were sieved through a 325 mesh (44 μm) and brushed onto kapton tape.

[a]Electronic mail: graetz@bnl.gov

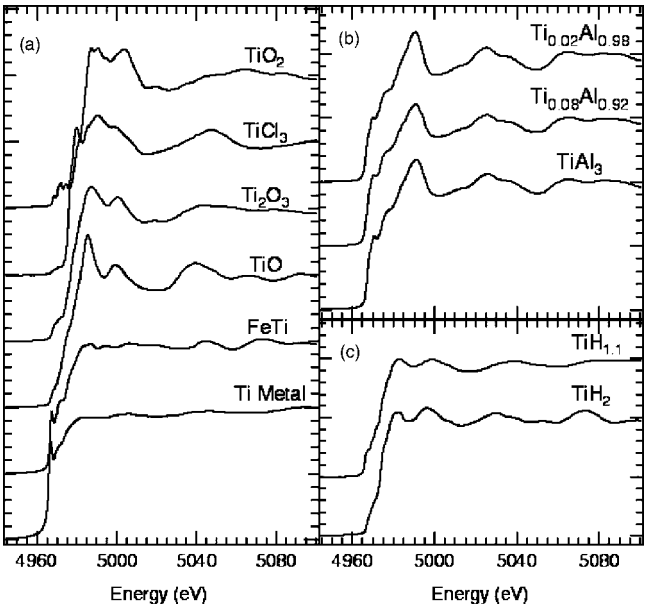

FIG. 1. (a) Ti *K* edges from Ti metal, FeTi, TiO, Ti_2O_3, $TiCl_3$, and TiO_2, (b) $TiAl_3$, nonstoichiometric $Ti_{0.08}Al_{0.92}$, and $Ti_{0.02}Al_{0.98}$, and (c) TiH_2 and nonstoichiometric $TiH_{1.1}$.

Ti *K*-edge spectra were collected at beamline X-19A at the National Synchrotron Radiation Light Source (NSLS) using a Si(111) double crystal monochromator. The higher-order harmonics were suppressed by detuning the second crystal of the monochromator on its rocking curve to 50% of the maximum transmitted intensity 400 eV above the edge. Spectra were recorded in fluorescence yield using a passivated implanted planar silicon detector for the reasonably concentrated samples and a 13-element Ge detector (Canberra) with an energy resolution of 240 eV for the diluted samples. All samples were kept at room temperature and oriented to have the incident x ray striking the surface at $45° \pm 5°$. This geometry provided essentially bulk-sensitive measurements. Due to small Ti concentrations, the near-edge spectra were not corrected for "self-absorption." The energy scale was calibrated by assigning $E = 4966$ eV to the first inflection point of the pure Ti foil within error of less than 0.1 eV. Air-sensitive samples were measured in a sealed sample holder after being loaded in a glove box under Ar. All spectra were background subtracted and normalized to a 100 eV window, 100 eV above the edge onset.

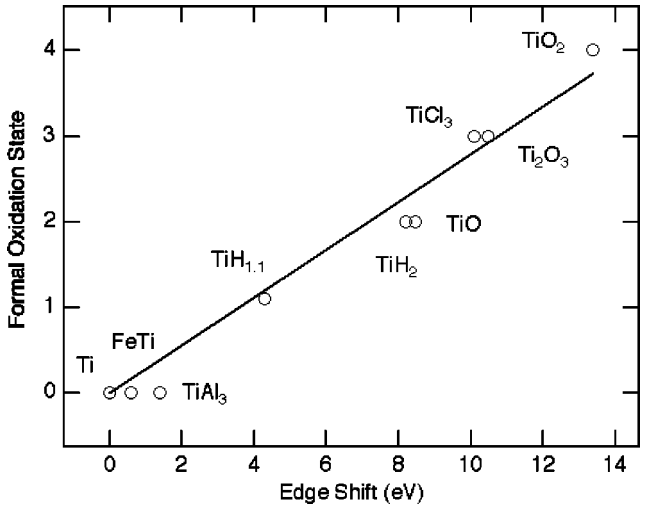

FIG. 2. Shift in the Ti *K*-edge onset energy with respect to the formal oxidation state in a series of Ti standards.

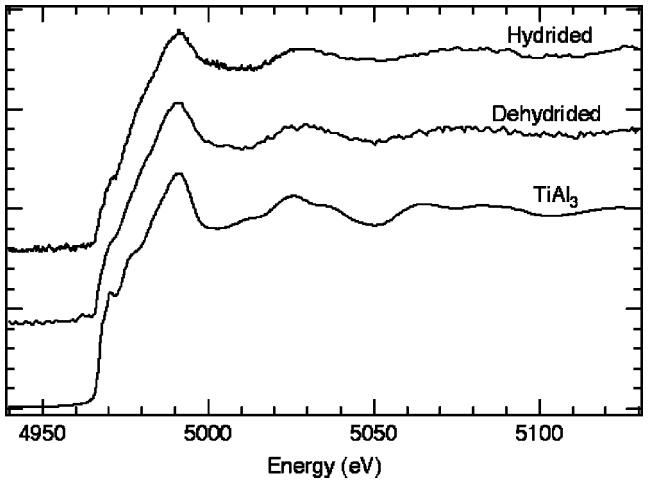

FIG. 3. Ti *K* edges from $TiAl_3$ and 2 mol % Ti-doped sodium alanate in hydrided and dehydrided states.

Powder x-ray diffraction (Rigaku Miniflex) of the Ti-doped $NaAlH_4$ after mechanical attrition revealed the presence of $NaAlH_4$ with some minor concentrations of α-Na_3AlH_6, metallic Al, and NaCl. A small amount of NaCl is initially formed upon ball milling, which results in the decomposition of a small amount of $NaAlH_4$. X-ray diffraction of the cycled samples suggests that additional NaCl and Al metal is formed upon cycling. The majority species in both dehydrided samples were NaH and metallic aluminum, consistent with Eq. (1). The hydrided 2 mol % Ti sample consisted of predominately $NaAlH_4$, whereas the 4 mol % Ti material exhibited more of a mixed phase, with $NaAlH_4$ and minor concentrations of αNa_3AlH_6 and metallic Al, suggesting the hydrogenation did not go to completion in this sample.

The Ti *K* edges from a series of Ti standards are displayed in Fig. 1(a). The Ti edges for $TiAl_3$ and two Al samples with 2 and 8 mol % Ti are shown in Fig. 1(b). The edges from the three different Ti concentrations are qualitatively identical. This is not surprising, since Ti is immiscible in Al at room temperature and will nucleate the $TiAl_3$ phase even at low dopant levels.[10,11] The Ti *K* edges from TiH_2 and $TiH_{1.1}$ [Fig. 1(c)] are also very similar, indicating that the structural environment around the Ti is essentially the same. However, the local disorder in the substoichiometric compound ($TiH_{1.1}$) is clearly visible above the edge.

The most interesting features in Fig. 1 are the large chemical shifts in the Ti *K* edge, relative to Ti metal. The shift of the Ti *K* edge reflects changes in the binding energy of the Ti 1*s* electron. The largest observed shift is about 13 eV between Ti metal, containing neutral Ti atoms, and TiO_2, containing Ti^{4+}. The increase in the 1*s* binding energy is due to reduced screening of the nuclear charge as the outer electrons are pulled off the atom.

A plot of the relationship between the edge onset and the formal Ti valence is shown in Fig. 2. The onset of the *K* edge was defined by the maximum of the first derivative. In cases where the peak in the first derivative was clearly split, such as in $TiH_{1.1}$, the onset was chosen as the midpoint between the two peaks. There is a linear correlation between the oxi-

TABLE I. Measured Ti *K*-edge onset energies and corresponding formal oxidation states for Ti-doped sodium alanates.

Dopant (mol %)	Condition	Edge shift (eV)	Oxidation state
4 Ti	Dehydrided	0.6	0.17 ± 0.01
4 Ti	Hydrided	1.3	0.36 ± 0.01
2 Ti	Dehydrided	1.9	0.53 ± 0.02
2 Ti	Hydrided	1.9	0.53 ± 0.02

dation state of the Ti ion, n, and the edge shift with respect to Ti metal, ΔE. This relationship ($n = c\Delta E$) has a coefficient of $c = 0.28 \pm 0.01$.

The edge onset energies were used to determine the formal Ti valence in the Ti-doped sodium alanates and the results are displayed in Table I. In the hydrided and dehydrided compounds the Ti is essentially zero valent (total charge transfer of half an electron, or less). Although the neutral character of the Ti valence is supported by a number of other studies,[1,5–7,12] this is direct evidence of zero-valent Ti at dopant levels of 2–4 mol %. The Ti *K* edge from the as-milled material is believed to be the superposition of edges and, therefore, no oxidation states were calculated.

The structure of the Ti *K* edge can also be used to gain insight into the local Ti environment. Figure 3 displays a plot of the Ti *K* edge from the hydrided and dehydrided 2 mol % Ti-doped sodium alanates and $TiAl_3$. In the doped sodium alanates, a small shoulder is evident just above the main peak (4998–5010 eV), which may be attributed to the presence of a small amount of nearby hydrogen. The formation of titanium hydride is not unlikely since the presence of any Ti metal would likely form TiH_{2-x} during the first desorption. Despite this minor difference, the fine structure above the edge (4960–5100 eV) is qualitatively similar for the Ti-activated alanates and $TiAl_3$. This suggests that the Ti is coordinated by Al atoms and that the local order is similar to that of $TiAl_3$. This is not surprising since $TiAl_3$ is the most thermodynamically favorable Ti product ($\Delta H_{298\ K} = -142.4$ kJ/mol),[13] followed by TiH_2 ($\Delta H_{298\ K} = -119.7$ kJ/mol)[14] and Ti_3Al ($\Delta H_{298\ K} = -100.5$ kJ/mol).[13] However, the oscillations are clearly less pronounced in the doped alanates, suggesting that the Ti lacks the long-range order that exists in crystalline $TiAl_3$. This supports the recent study of Weidenthaler *et al.* that demonstrated that Ti is atomically dispersed and essentially amorphous in this system.[15] The lack of long-range order would also explain why $TiAl_3$ has never been directly observed at these dopant levels through diffraction techniques.

The Ti *K* edge of the mechanically milled material (no cycling) exhibits peaks at 4988 and 4998 eV (Fig. 4). This structure may be indicative of the superposition of edges from Ti in multiple environments, the initial $TiCl_3$, TiH_{2-x}, and possibly $TiAl_3$. The decomposition of $NaAlH_4$ during mechanical milling liberates Al and H_2, either of which may form a compound with Ti. Although $TiAl_3$ is more stable, the liberated H_2 is considerably more mobile and therefore more likely to react with Ti and form TiH_{2-x}. It is likely that the formation of $TiAl_3$ predominantly occurs during the first decomposition, where metallic Al is more abundant.

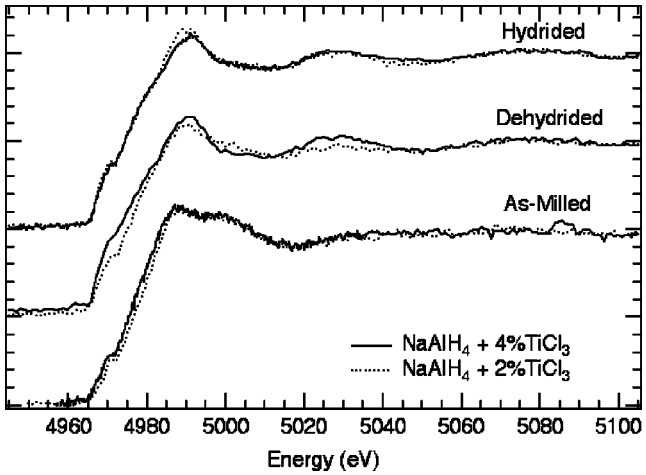

FIG. 4. Ti *K* edges from sodium alanate doped with 2 (thin line) and 4 mol % Ti (thick line). Edges are shown for the mechanically milled material (no cycling) and the dehydrided and hydrided material after four cycles.

A final interesting feature of Fig. 4 is the similarity of the hydrided and dehydrided spectra. This suggests that the local environment around the Ti is nearly invariant during the hydrogen cycle [Eq. (1)]. Although there is no long-range order, the Ti is locally coordinated by Al at every stage of the reaction.

These results confirm that the Ti is not present in the form of Ti metal and clearly demonstrate that there is no bulk lattice substitution. The catalyzing agent in Ti-doped $NaAlH_4$ is present on the surface in the form of amorphous $TiAl_3$.

This work was supported by U.S. DOE Contract No. DE-AC02-98CH10886 and NSF Contract No. DMR-0216858.

[1] B. Bogdanovic and M. Schwickardi, J. Alloys Compd. **253–254**, 1 (1997).
[2] K. J. Gross, S. Guthrie, S. Takara, and G. Thomas, J. Alloys Compd. **297**, 270 (2000).
[3] D. Sun, T. Kiyobayashi, H. T. Takeshita, N. Kuriyama, and C. M. Jensen, J. Alloys Compd. **337**, L8 (2002).
[4] G. M. Jensen and R. Zidan, Int. J. Hydrogen Energy **24**, 461 (1999).
[5] G. J. Thomas, K. J. Gross, N. Y. C. Yang, and C. Jensen, J. Alloys Compd. **330–332**, 702 (2002).
[6] B. Bogdanovic, R. Brand, A. Marjanovic, M. Schwickardi, and J. Tolle, J. Alloys Compd. **302**, 36 (2000).
[7] E. H. Majzoub and K. J. Gross, J. Alloys Compd. **356–357**, 363 (2003).
[8] G. Sandrock, K. J. Gross, G. Thomas, C. Jensen, D. Meeker, and S. Takara, J. Alloys Compd. **330–332**, 696 (2002).
[9] R. A. Zidan, S. Takara, A. G. Hee, and C. M. Jensen, J. Alloys Compd. **285**, 119 (1999).
[10] *Binary Alloy Phase Diagrams*, edited by R. D. Massalski (ASM International, Metals Park, OH, 1990), Vol. 1.
[11] K. J. Gross, E. H. Majzoub, and S. W. Spangler, J. Alloys Compd. **356**, 423 (2003).
[12] V. P. Balema, J. W. Wiench, K. W. Dennis, M. Pruski, and V. K. Pecharsky, J. Alloys Compd. **329**, 108 (2001).
[13] C. J. Smithells, *Metals Reference Book*, 4th ed. (Butterworth, London, 1967).
[14] *Handbook of Chemistry and Physics*, 64th ed. (Chemical Rubber, Press, Boca Raton, FL, 1983).
[15] C. Weidenthaler, A. Pommerin, M. Felderhoff, B. Bogdanovic, and F. Schuth, Phys. Chem. Chem. Phys. **5**, 5149 (2003).